LU TP 01-02
January 2001

GRAVITY IN EXTRA DIMENSIONAL SPACES

Master of Science Thesis by Anders Månsson

Thesis Advisors: Johan Bijnens, Martin Maul

Department of Theoretical Physics,
Lund University, Lund, Sweden

Abstract

Despite the fact that the Standard Model (SM) of strong and electroweak interactions successfully describes all observed phenomena at currently accessible energies $M_W \sim 100$ GeV, where M_W is the electroweak scale, there are several indications for new physics beyond the SM to exist. It is widely believed that an unified theory of all fundamental forces in nature can be consistently constructed in space-time with more than four dimensions.
In the first part of this article we will analyze the possibility of measuring a change in the maximum mass of a white dwarf and a neutron star in spaces with 1-6 relatively large extra dimensions.
In the second part of this article we present a way of measuring a spectrum of massive graviton resonances, that the Randall-Sundrum model predicts, in an experiment that could be performed at the upcoming ATLAS and CMS program at LHC, starting in the year 2005.

Contents

1 Introduction

The concept of higher-dimensional spaces is based on some of the most recent developments in string theory. The assumption is that everything we can see in our universe is confined to a four-dimensional "wall" or "membrane" that lies within a higher-dimensional realm, where the extra dimensions are supposed to be curled up into small circles. Only the graviton (the postulated force transmitter for gravity) is allowed to move in the extra dimensions. One of the recent major breakthroughs in string theory has been the recognition that the theory contains the above mentioned walls, known as D-branes, where "brane" comes from the word "membrane" and "D" stands for "Dirichlet", which indicates a mathematical property of the branes.

One reason for assuming the existence of extra dimensions was that one wanted to explain why gravity is so much weaker than the other known forces and to explain the huge mass gap between the graviton and all other known particles. If the graviton exists its mass would be about $\sqrt{G} \approx 10^{19}$ GeV (Planck scale) and all other known particles have masses of about 1 TeV or smaller. (In length units the Planck scale is approximately 10^{-35} meter.)

Because gravity becomes comparable in strength to electromagnetism and the other forces at the Planck scale, physicists have traditionally assumed that the theory unifying gravity with other interactions could reveal itself only at these energies. The presence of extra space dimensions makes gravity stronger at shorter distances. This lowers the energy Planck scale and also the mass of the graviton. By postulating enough extra dimensions the Planck scale and the graviton mass come very close to the electroweak scale. The unification of all forces could then take place near 10^{-19} meter rather than 10^{-35} meter. How many extra dimensions are needed depends on how large they are. Conversely, for a given number of extra dimensions one can compute how large they must be to make gravity strong near 10^{-19} meter.

In the first part of this diploma work we will consider spaces with 1-6 extra dimensions, with a relatively large radius ($R \approx 1$ mm for two extra dimensions). For these spaces we will calculate the maximum mass a white dwarf and a neutron star can have before they collapse under the effect of gravity. We will compare these maximum masses to the maximum masses one obtains in a normal space with three dimensions (excluding time).

In the second part of this diploma work we will consider a different situation. We will work with the Randall-Sundrum model, which deals with only one, very small, extra dimension ($R \approx 10^{-32}$ m). The Randall-Sundrum model predicts a spectrum of narrow massive graviton states that are well separated in mass and can be detected as resonances in collider experiments. This is one of the tasks for the upcoming ATLAS detector at the Large Hadron Collider (LHC) at CERN. We will present a simulated experiment for the ATLAS detector at the LHC and by considering a so called $p_\perp$-spectrum one could find signs of the gravitational resonances that the Randall-Sundrum predicts.

2 Extra dimensions in neutron stars and white dwarfs

The presence of compactified, extra dimensions changes radically the gravitational force at small distances. At this scale it becomes much stronger than the classical Newton force. So if the extra dimensions exist, there might be a possibility to observe changes in physical phenomena that significantly depend on gravitation at small scales. One possible area where one could observe differences from existing measurements is in astronomy and the observation of stars. A star's structure depends of course significantly on gravitation and the particles making up the star can come very close to one another if the star is hot enough.

In the first part of this work we will analyze the possibility to observe a change in the maximum mass a star can have before it collapses. One would only expect a small change in the mass, because otherwise one would already have found discrepancies from existing observation data. But still the changes could be relatively large, because astronomical measurements are often connected with relatively large uncertainties, due to the large distances and the technical difficulties in the measurements.

2.1 A brief introduction to stellar evolution

A shining star is radiating a lot of energy by light emission. It is nuclear fusion processes, mainly the conversion of hydrogen to helium in an ordinary star like our Sun, that replaces the lost energy in order for the star to remain static. During the conversion of the original supply of hydrogen into helium, this energy source decreases with time and the inner region of the star, the core, begins to shrink as it gradually radiates energy away. This shrinking compresses and heats the core, until the temperatures are high enough to ignite another reaction which converts helium into carbon and oxygen, releasing more energy. As a result of the release of this new energy, the outer layers of the star expand dramatically and the star has become a so called red giant. After some time all the helium have been used up and the star may then go through phases of turning carbon into silicon, and silicon into iron. Eventually, every star must run out of energy, since iron is the most stable of all nuclei and any reaction converting iron into something else just absorbs energy rather than releasing it. The precise time when this happens and the subsequent evolution of the star depend mainly on three things: the star's mass, angular momentum and magnetic field.
Let us first consider a slowly rotating star. Here the rotation is not an important factor for the structure of the star. A star with the mass of the Sun will by evolving smoothly eventually become a so called white dwarf. The pressure of this star does not only come from thermal effects but also from quantum mechanical ones, as will be discussed more in detail later. The point about relatively low-mass stars like our Sun is that they do not have strong enough gravitational fields to overwhelm these quantum effects or to cause rapid contraction earlier on in their history.
A higher-mass star will also evolve smoothly through the hydrogen-burning phase (called

the “main sequence” phase), but what happens after that is not completely understood. Massive stars are known to have strong stellar winds which can cause the loss of considerable fractions of their mass during the main-sequence stage. Stars in close binary systems may also pass considerable mass to their companions as they evolve off the main sequence. If a star loses enough mass, its subsequent evolution may be quiet, like that expected for our Sun. But if the star is not able to lose enough mass, it is believed that it will undergo a supernova explosion. (Avoiding going into details, let us just say that this could be substantially altered by such things as rotation and magnetic fields.) A supernova often leaves behind rapidly rotating neutron stars, which are observed as pulsars.
This ends our short introduction of how white dwarfs and neutron stars comes about.

2.2 Ideal gas

In the following, when working with the white dwarf and the neutron star, we will assume that we can treat them as ideal gases, that is we do not consider other interactions than gravity. We are treating the particles as point-like. Some of the particles under consideration will be Fermi particles and therefore they obey Pauli's exclusion principle.

2.3 Static stars

In a star, the pressure from the hot gas of particles making up the star balances the inward pulling force due to gravitation. Pressure is due to the internal motion of particles in the gas, including such force-transmitting particles as photons and neutrinos. As some particles in the gas are fermions, the lowest obtainable pressure will be different from zero, due to Pauli's exclusion principle that forbids two identical fermions to be in the same state.
According to the uncertainty relation one will have an uncertainty in the momentum of a particle, when it is confined to a region of volume V, by an amount of the order:

$$\Delta p \approx hV^{-1/3}. \tag{1}$$

The particle will then fill up a volume Δp in momentum space, around some momentum point (p_x, p_y, p_z). Because we are considering fermions and they obey Pauli's exclusion principle, we cannot have overlap between wave functions. This means that even at the lowest possible total energy state ($T = 0$), they will occupy all momentum states up to some momentum p_{F}. Though the star contracts under gravity and gradually cools by giving off radiation, there will always be some pressure supplied by the fermions. If the star's mass is not too large, the star will then stop contracting and the pressure will balance the gravitation of the star. Considering a star, in our case with constant density, there will be an upper limit to the mass that can be supported by the star's internal pressure. For a white dwarf this maximum mass is called the Chandrasekhar mass, M_{Ch}. But since we also are going to calculate it for a neutron star, we will more generally call it the "maximum mass" or M_{max}. In the first part of this diploma work, we will calculate the maximum mass of a white dwarf and a neutron star for a (3+d)-dimensional space (excluding time). To do this we first have to see how the gravitational potential looks in this kind of space.

2.4 Gravity in a n-dimensional Euclidean space

Let us consider a static, 3-dimensional, Euclidean space. In classical physics the potential between two point-like masses m_1 and m_2 at distance r from each other is given by

$$V(r) = -G\frac{m_1\, m_2}{r}. \tag{2}$$

We now want to generalize the potential to the case of n spatial dimensions.

One can motivate in several ways a formula for the potential between two point-like masses m_1 and m_2 at distance r from each other in a n-dimensional space. One can motivate it more strict mathematically, but we will motivate it in an intuitive way. First we will see how the potential looks for 1, 2 and 3 spatial dimensions. From this one can generalize it to a higher dimensional space.

Consider gravitational flux lines going into a point-like mass placed at the origin. The force on a massive surface element at some point is proportional to the number of flux lines passing through the surface element. Thus the gravitational force on the surface element is proportional to the gravitational flux density, which is the number of flux lines going through the surface element divided by its "area".

In 1 dimension the gravitational flux can only go in two directions and the perpendicular surface element will be a point. Of course a point does not have an "area", but since there is exactly one flux line going through each point, the force will (by convention) be constant:

$$F = \text{constant},\ V \propto r \tag{3}$$

where F is the force and V the potential. (One can motivate the 1-dimensional case better if one considers a 1-dimensional space with 1 extra, compactified dimension; see next section.)

In 2 dimensions we have radial flux lines as shown in fig. 1. The perpendicular "surface-area" is here given by a small arc length on a circle of constant r. Since the same number

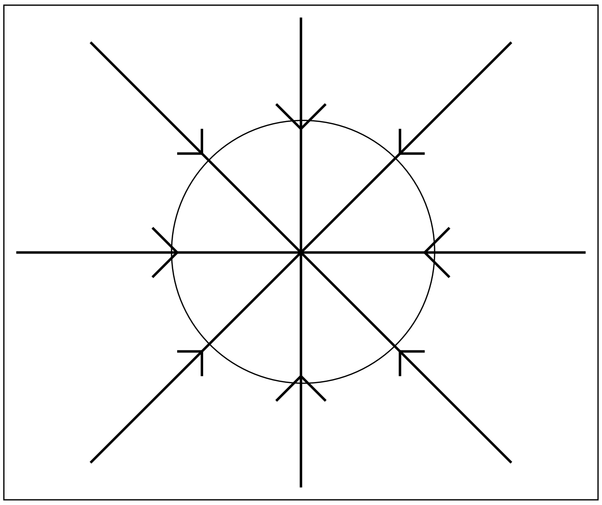

Figure 1: Radial flux lines into a point-like mass in 2 dimensions.

of radial flux lines goes through every circle and the arc length goes as r we have:

$$F \propto \frac{1}{r},\ V \propto \ln r. \tag{4}$$

In 3 dimensions the surface element is a part of a sphere of radius r and the flux lines are radial lines. Here the area goes as r^2, so we get:

$$F \propto \frac{1}{r^2},\ V \propto \frac{1}{r}. \tag{5}$$

It is now easy to generalize the potential in $n \geq 3$ dimensions:

$$F \propto \frac{1}{r^{(n-1)}},\ V \propto \frac{1}{r^{(n-2)}}. \tag{6}$$

2.5 Compactified extra dimensions

Now that we have an expression for the potential in an Euclidean space of n dimensions, we can find the potential for a 3-dimensional Euclidean space with d compactified and identical extra dimensions. To do this we will generalize the case of a 1-dimensional space with 1 extra compactified dimension. As we will soon see, one will have two completely different behaviors of the gravitational force at small respectively at large distances.

Assume that the extra dimension is a circle with radius R, as shown in fig. 2. Close

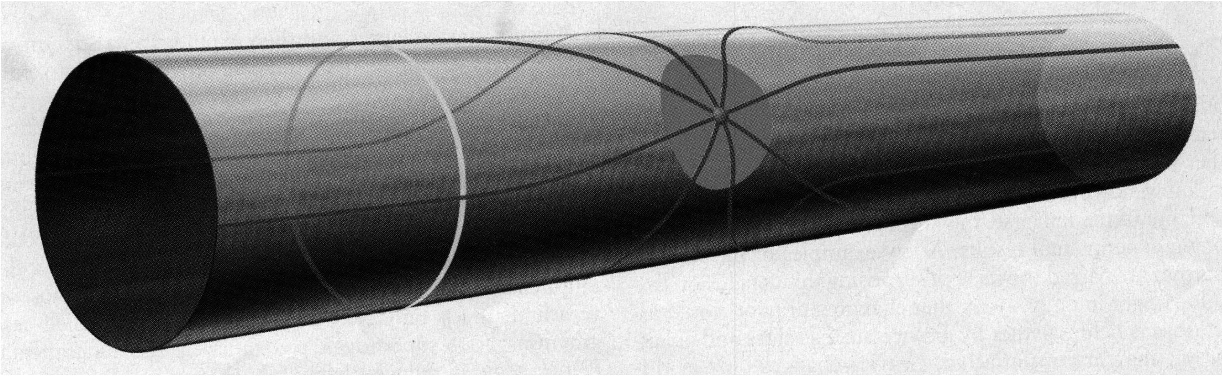

Figure 2: A 1-dimensional space with one extra, compactified dimension. The lines are the gravitational flux lines from a point-like mass. In the small circle-area around the mass, the potential is like that belonging to a 2-dimensional Euclidean space. At the light circle further down the cylinder the potential is like that belonging to a 1-dimensional Euclidean space. [The picture is taken from Scientific American, August 2000]

to the mass point the space looks flat, approximately Euclidean, and the behavior of the potential can be determined as above for 2 dimensions ($V \propto \ln r$). For distances $r \gg R$ the flux lines will align themselves in the direction of the cylinder and the flux density will be practically constant, and as for the 1-dimensional case we get $V \propto r$.

2.6 The (3+d)-dimensional gravitation potential

It is now easy to generalize the potential to the case of (3+d) dimensions. For small distances away from the mass point we will have $V \propto r^{-(d+1)}$ and for large distances we will have a classical Newtonian potential behavior, that is $V \propto r^{-1}$.

We have thus determined the asymptotic behavior of the potential. It remains to determine the behavior of the potential for intermediate r, to match the two asymptotic expressions. An assumption we now make is that the exact behavior of the potential for r of the order of R should not matter significantly. It is rather the strong short distance behavior of the potential that gives the main contribution to the extra-dimensional part of the total potential of a star, to be calculated later. We therefore choose a starting potential that has a natural connection between the two limiting potentials and which will give simple calculations.
The starting potential for two point-like masses m_1 and m_2 at a distance r from each other is

$$V(r) = -\frac{Gm_1m_2}{R}\sqrt{\frac{R^2}{r^2+R_E^2}}\left[1 + C\left(\frac{R^2}{r^2+R_E^2}\right)^{d/2}\right] = -Gm_1m_2\mathcal{V}(r). \qquad (7)$$

As before d is the number of extra dimensions and G is the gravitation constant. R is the radius of the extra dimensions and R_E is the so called cut-off constant, which changes the potential at the value $R_E > 0$ and thereby prevents integrals from diverging. This means physically that we do not care about what happens for energies that correspond to smaller values than R_E. We will come back to this point when we do the numerical calculations of the corrections to the maximum mass.
$C = O_3/[(d+1)O_n]$ is a constant that has its origin in the Poisson equation [1]; $O_n = 2\pi^{n/2}/\,\Gamma[n/2]$, where n is the number of space dimensions (including extra dimensions) and Γ is the Gamma function.

2.6.1 Massive gravitons

One can also motivate eq. (7) with the exchange of massive gravitons, in Kaluza-Klein formalism.
Consider a static one dimensional space with one extra dimension, where the extra dimension is a circle of radius R (see fig. 2). Let us consider a plane wave of a graviton in this (1+1)-dimensional space, where the ordinary dimension is denoted by x, the extra dimension is denoted by y and k is the wave vector:

$$\psi(x,y,t) \propto e^{i(k_x x + k_y y - \frac{Et}{\hbar})}. \tag{8}$$

If one wants to have a single valued function, the following condition has to be satisfied:

$$e^{ik_y(2\pi R)} = 1 \;\Leftrightarrow\; k_y = \frac{n}{R} \tag{9}$$

where n is an integer. The energy of the graviton is then given by:

$$E^2 = p_x^2c^2 + p_y^2c^2 = p_x^2c^2 + \hbar^2c^2\frac{n^2}{R^2}. \tag{10}$$

If $n = 0$, the energy looks like it belongs to a massless particle with wave vector $k_x = p_x/\hbar$. If $n \neq 0$, the graviton will also have motion in the extra dimension. But we cannot "see" the graviton propagating in the extra dimension, since we are stuck to our D-brane. The point is now, remembering that the energy of a particle is given by the relation

$$E^2 = p^2c^2 + m^2c^4, \tag{11}$$

that we can interpret the second term in eq. (10) as if the graviton had a mass

$$m_n = \frac{\hbar}{c}\frac{\sqrt{n^2}}{R}. \tag{12}$$

This expression for the graviton mass is easily generalized to a space with d extra dimensions, just by doing the substitution:

$$\sqrt{n^2} \;\rightarrow\; \sqrt{n_1^2 + ... + n_d^2} \;\Rightarrow\; m_{\vec{n}} = \frac{\hbar}{c}\frac{\sqrt{n_1^2 + ... + n_d^2}}{R}. \tag{13}$$

If one had a quantum field theory for gravity with the graviton G as an exchange particle, one would have the following general expression for the gravitational potential:

$$V_G = \sum_{\vec{n}} \frac{\mathrm{e}^{-m_{\vec{n}} r}}{r}. \tag{14}$$

One can show that this is actually the same generalized potential as in eq. (6).

2.7 Total potential energy of a homogeneous star

To calculate M_{max} we will use the total energy of the star. Let us first calculate the total potential energy of the star. Using eq. (7) we can compute the total potential energy of a star with radius L and constant mass density ρ, which includes the mass contribution from the kinetic energy of the particles (given by Einstein's mass-energy relation, $m = E/c^2$). Since the particles are confined to the D-brane, the integration is over the normal 3-dimensional space:

$$E_{\mathrm{pot}}^{(d)} = -\frac{G\rho^2}{2} \int_{B(L)} d^3\mathbf{r} \int_{B(L)} d^3\mathbf{r}' \; \mathcal{V}(|\mathbf{r} - \mathbf{r}'|) \; . \tag{15}$$

Technically for the calculation one can make use of the trick that for an integer n one has

$$\begin{aligned} \left(\sqrt{\frac{R^2}{r^2 + R_E^2}}\right)^{2n+1} &= \frac{(-2R^2)^n}{(2n-1)!!}\frac{d^n}{d\alpha^n}\bigg|_{\alpha=R_E^2} \sqrt{\frac{R^2}{r^2+\alpha}} \\ \left(\frac{R^2}{r^2 + R_E^2}\right)^{n+1} &= \frac{(-R^2)^n}{(n!)}\frac{d^n}{d\alpha^n}\bigg|_{\alpha=R_E^2} \frac{R^2}{r^2+\alpha}. \end{aligned} \tag{16}$$

We then get the total potential energy of a star with constant density, with mass M and radius L, using that R_E is very small and only keeping the R_E-terms $\ln(R_E)$ and R_E^k where $k \leq 0$:

$$
\begin{aligned}
E_{\mathrm{pot}}^{(d=1)} &= -\frac{3GM^2}{5L} - C\frac{9GM^2R}{8L^2} \\
E_{\mathrm{pot}}^{(d=2)} &= -\frac{3GM^2}{5L} - C\frac{GM^2R^2}{2L^3}\left[3\ln\left(\frac{4L}{R_E}\right) - 7\right] \\
E_{\mathrm{pot}}^{(d=3)} &= -\frac{3GM^2}{5L} - C\frac{3GM^2R^3}{8L^4}\left[\frac{\pi L}{R_E} - 3\ln\left(\frac{2L}{R_E}\right)\right] \\
E_{\mathrm{pot}}^{(d=4)} &= -\frac{3GM^2}{5L} - C\frac{GM^2R^4}{L^5}\left(\frac{L^2}{2R_E^2} - \frac{3L}{4R_E} + \frac{9}{16}\right) \\
E_{\mathrm{pot}}^{(d=5)} &= -\frac{3GM^2}{5L} - C\frac{GM^2R^5}{128L^6} \\
&\quad \times \left[12\pi\frac{L^3}{R_E^3} - 36\frac{L^2}{R_E^2} + 12\ln\left(\frac{2L}{R_E}\right) + 1\right] \\
E_{\mathrm{pot}}^{(d=6)} &= -\frac{3GM^2}{5L} - C\frac{GM^2R^6}{L^7} \\
&\quad \times \left[\frac{L^4}{5R_E^4} - \frac{3L^3}{20R_E^3} + \frac{L}{20R_E} - \frac{3}{128}\right]. \qquad (17)
\end{aligned}
$$

The first term in all these expressions is the total potential energy without extra dimensions (put $C = 0$ and let $R_E \to 0$). The second term (containing C) is assumed to be small compared to the first term and it is the contribution from the extra dimensions.

2.8 White dwarfs

Let us consider an ordinary star that has been compressed under gravity and become a white dwarf, and that has reached a stage where one effectively has two gases, one of electrons and one of nuclei. Upon compression the Fermi momentum rises until it becomes comparable with the momentum of the electrons. They are then effectively a cold electron gas and supply the pressure for the star.
Gradually the star will cool by emitting radiation and some stars will eventually cool so much that the nuclei move very slowly. Because the electrons form a Fermi gas, they will even at zero temperature have some distribution in momentum up to the Fermi momentum p_{F}. So we will finally have a situation where the electrons have much larger kinetic energy than the nuclei. On the other hand, the nuclei supply most of the gravity, since the nuclei are much more massive than the electrons.

2.8.1 Energy of the electron gas

As mentioned earlier, each electron will occupy some volume in momentum space, due to the uncertainty relation and Pauli's exclusion principle. If we assume that the electron gas is as cool as possible, they will fill all momentum states up to the momentum magnitude p_{F}. Remembering that every electron can have either spin up or spin down, which doubles the number of states that the electrons can occupy, the number of electrons dN in the interval $[p, p+dp]$ is given by

$$dN = 2\,\frac{4\pi p^2 dp}{(\Delta p)^3} = \frac{8\pi p^2 dp}{h^3}V. \tag{18}$$

The number density of electrons n_e is then given by

$$n_e = \frac{N}{V} = \int_0^{p_{\mathrm{F}}} \frac{8\pi p^2 dp}{h^3} = \frac{8\pi p_{\mathrm{F}}^3}{3h^3}. \tag{19}$$

On the other hand we also have that

$$n_e = \frac{\rho}{\mu m_p}, \tag{20}$$

where μ is the ratio of number of nucleons to the number of electrons, m_p is the proton mass (the nucleon mass) and ρ is the mass density of the white dwarf. In the equation above we have only considered mass contributions from the rest masses of the nuclei. All other mass contributions we assume to be small enough so that we can neglect them.

The energy of one electron is $E = (m_e^2c^4 + p^2c^2)^{1/2}$ and because we are considering a very dense electron gas we assume that $p_{\mathrm{F}}c \gg m_ec^2$. This inequality can be written in terms of the radius L and mass M by using eq. (19) and eq. (20):

$$L \ll \alpha M^{1/3} \text{ where } \alpha = \frac{h}{m_e c}\left(\frac{9}{32\pi^2\mu m_p}\right)^{1/3}. \tag{21}$$

We can now get a relation between the total (rest mass + kinetic)-energy E_e of the electron gas on one side, and the mass M and radius L on the other:

$$\begin{aligned} E_e &= \rho_e V = V\int_0^{p_{\mathrm{F}}} \frac{8\pi p^2}{h^3}(m_e^2c^4 + p^2c^2)^{1/2}dp \\ &\approx V\int_0^{p_{\mathrm{F}}} \frac{8\pi c p^3}{h^3} = V\frac{2\pi c}{h^3}p_{\mathrm{F}}^4 = V\frac{2\pi c}{h^3}\left(\frac{3h^3\rho}{8\pi\mu m_p}\right)^{4/3} \\ &= \left(\frac{3^5h^3c^3}{2^{11}\pi^2\mu^4m_p^4}\right)^{1/3}\frac{M^{4/3}}{L} \end{aligned} \tag{22}$$

where ρ_e is the (rest mass+kinetic)-energy density of the electrons.

2.8.2 The total energy of the white dwarf

Finally we get the total energy of a star:

$$E_{tot}^{(d)} = E_n + E_e + E_p^{(d)} \approx E_m + E_e + E_p^{(d)}. \tag{23}$$

Here n stands for nuclei, e for electron, p for potential, m for total rest mass of the nuclei and d is the number of extra dimensions. In the second equality have we neglected the kinetic energy of the nuclei.

Because we only are going to study the shape of the graph of $E_{tot}^{(d)}$, by varying L and keeping M constant, we can forget about terms in $E_{tot}^{(d)}$ not depending on L. This means that we can skip the term E_m in $E_{tot}^{(d)}$, because this only depends on M. So instead we consider the following expression for $E_{tot}^{(d)}$ as the total energy of the star:

$$E_{tot}^{(d)} = E_e + E_p^{(d)}. \tag{24}$$

Using that $L \gg R_E$ to keep only the largest term containing R_E in eq. (17) (one can treat the term inside the brackets for $E_{pot}^{(d=2)}$ as a positive constant), we will for all d have the following approximate general form of the equation for $E_{tot}^{(d)}$:

$$E_{tot}^{(d)} = \frac{\alpha_1 M^{4/3} - \alpha_2 M^2}{L} - \frac{\alpha_3 M^2}{L^k}. \tag{25}$$

α_1, α_2 and α_3 are positive constants not depending on M or L, and k is an integer larger than one.

We now see that there is no stable minimum of $E_{tot}^{(d)}$. As we will come back to later, a minimum of $E_{tot}^{(d)}$ has to do with the stability of the star. To find a minimum one also has to consider the behavior of the total energy of the star when the electrons are non-relativistic, which happens for larger values of the star's radius L (see eq. (21)). We will come back to this point later.

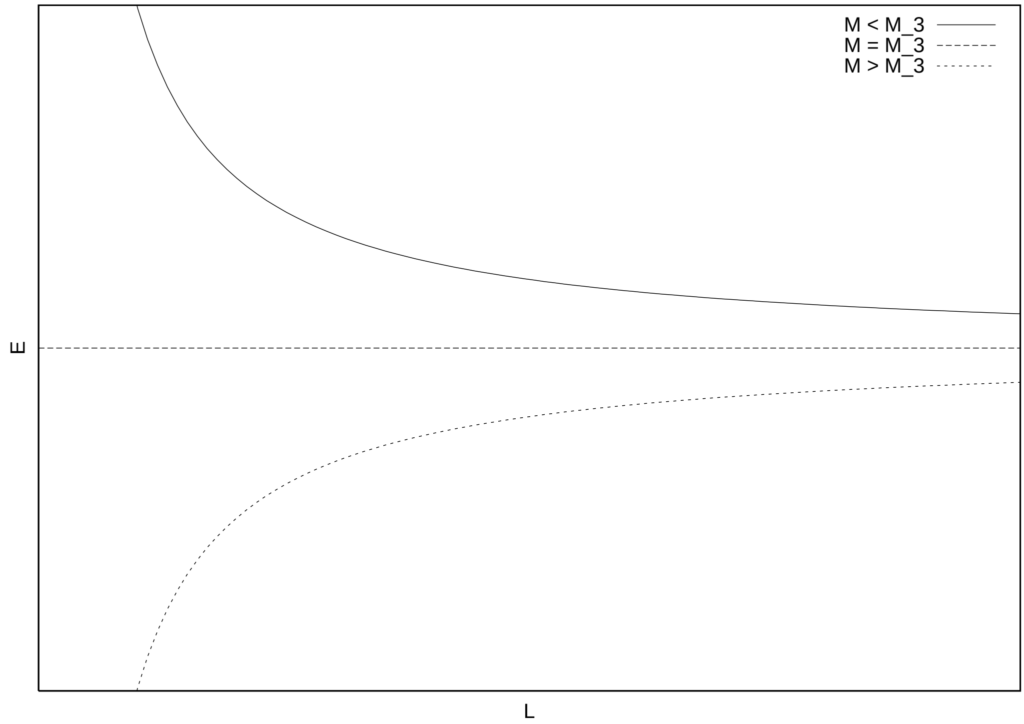

Figure 3: The general shape of the $E_{tot}^{(0)}$-curve.

2.8.3 Total energy curves for stars with $(T = 0)$

Assume that we are considering a star (white dwarf or neutron star) with temperature $T = 0$. This star with mass M and radius L corresponds to a point on one of the curves, either in fig. 3 or fig. 4. $E_{tot}^{(0)}$ is plotted in fig. 3 as a function of L, for different masses M. The curves in fig. 4 are $E_{tot}^{(d)}$ (eq. (25)) plotted as a function of L, for different masses M.

In this model we do not consider other interactions than gravitation. In fact processes of electromagnetic and weak interactions (neutron stars) are of importance as well. For example a star can cool by emitting photons or neutrinos. The total energy of the star then decreases and the star can in this way move down the energy curve to a new point where again $T = 0$.

2.8.4 Chandrasekhar mass of a white dwarf when $(d = 0)$

Let us first put $\alpha_3 = 0$. Then we get the total energy in the case of no extra dimensions. One sees that the total energy would be proportional to L^{-1} in this case. The total energy curve is shown in fig. 3 for three different values of M.

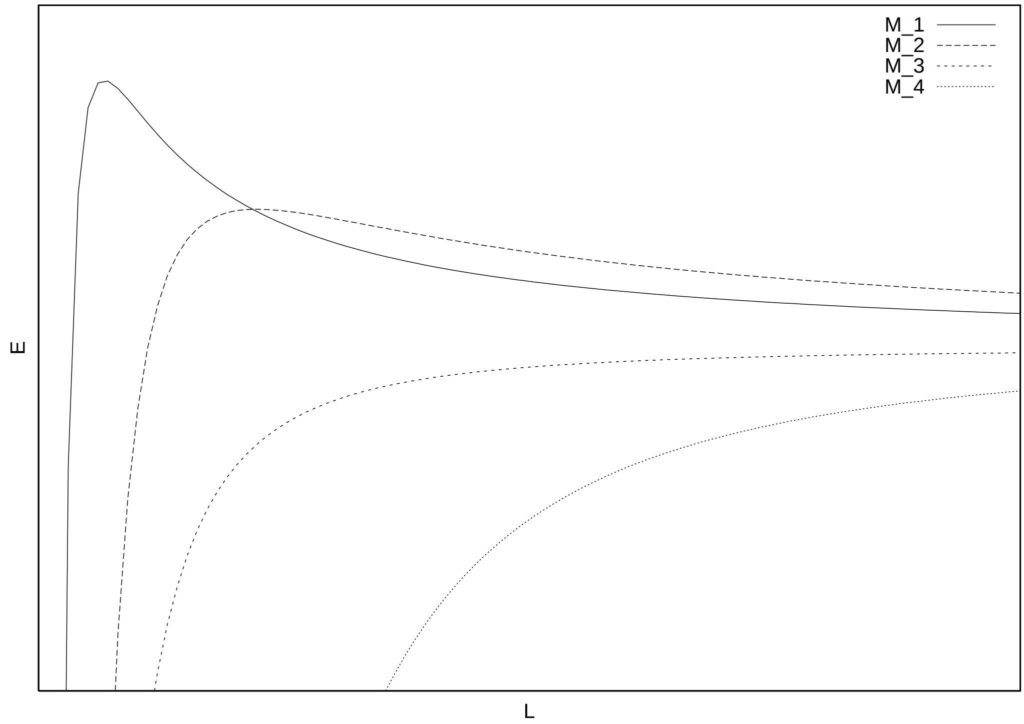

Figure 4: The general shape of the $E_{tot}^{(d)}$-curve. The greater the index is on M, the greater is the mass of the star.

$M = M_3$ in fig. 3 is here the M-value that makes the total energy identically equal to zero. (We call it M_3 to relate it to the mass in fig. 4, as will be discussed later.)
If $M > M_3$ the star move towards $L = 0$ no matter what L initially was, so the star is not stable and it will eventually collapse.
If $M < M_3$ then the star move towards larger values of L. If there is no minimum for larger L-values, outside the relativistic range, the star will expand forever. But since one actually observes seemingly stable white dwarfs (and neutron stars), one expects there to be something that stops the expansion for larger L (or that the expansion goes extremely slowly). We will therefore assume that there actually is a stable minimum of $E_{tot}^{(d)}$ for some L. Then the star can eventually become stable at some radius L, no matter what the radius initially was.

Thus M_3 is the Chandrasekhar mass, because it is the maximum mass the star can have if the star is to be stable.

2.8.5 Chandrasekhar mass of a white dwarf when ($d > 0$)

$E_{tot}^{(d)}$ from eq. (25) is plotted in fig. 4 as a function of L, for different values of M. The greater the index is on M in fig. 4, the greater is the mass of the star. One can see that for very large values of M, the curve will look like M_4. That is, the energy is monotonically decreasing when going to smaller L-values.
If we consider smaller values of M, then for some certain M-value the curve will look like that of M_3. This happens when

$$E_e + E_p^{(0)} = 0 \tag{26}$$

where $E_p^{(0)}$ is the total potential energy when there are no extra dimensions. For all $M < M_3$ there exists a finite L where the total energy has a maximum. Two examples are the curves M_1 and M_2 in fig. 4. Above we assumed that the energy will start to rise for larger L. This means that there will be a minimum somewhere between the maximum and the rise of the curve for larger L, if one also know that the maximum lies inside the relativistic L-range (see eq. (21)).

Let us now assume that we are considering a white dwarf, lying to the right of the maximum peak on for example M_1 in fig. 4. To lower its energy the white dwarf could start going down the M_1 curve, by emitting radiation (in the way that was described earlier). Of course the mass changes when it radiates, but we expect the loss in mass to be very small, so that we stay on M_1 all the time. Eventually the white dwarf becomes stable as we have a minimum somewhere to the right of the peak (not indicated in the figure).

If the white dwarf should be lying to the left of the maximum peak, there would be nothing to stop it from collapsing as this would be energetically beneficial. In this case the white dwarf is unstable.

The limiting case between the above two cases is when the star is exactly at the maximum. If we observe a stable white dwarf that has a radius L and T=0, the maximum peak should be to the left of L, inside the star, otherwise it would not be stable. So we get the maximum mass (Chandrasekhar mass) of the white dwarf when the maximum peak is at L, that is by solving:

$$\frac{\partial E_{tot}^{(d)}}{\partial L} = 0, \tag{27}$$

where one is treating M as a constant.

The Chandrasekhar mass is then given by:

$$\begin{aligned}
M_{\mathrm{Ch}}^{(d=1)} &= M_{\mathrm{Ch}}^{(0)}\left\{1 - C\frac{45}{8}\frac{R}{L}\right\} \\
M_{\mathrm{Ch}}^{(d=2)} &= M_{\mathrm{Ch}}^{(0)}\left\{1 - C\frac{15}{4}\frac{R^2}{L^2}\left[3\ln\left(\frac{4L}{R_E}\right) - 8\right]\right\} \\
M_{\mathrm{Ch}}^{(d=3)} &= M_{\mathrm{Ch}}^{(0)}\left\{1 - C\frac{45}{16}\frac{R^3}{L^3}\left[\frac{\pi L}{R_E} - 4\ln\left(\frac{2L}{R_E}\right) + 1\right]\right\} \\
M_{\mathrm{Ch}}^{(d=4)} &= M_{\mathrm{Ch}}^{(0)}\left\{1 - C\frac{15}{2}\frac{R^4}{L^4}\left(\frac{L^2}{2R_E^2} - \frac{L}{R_E} + \frac{15}{16}\right)\right\} \\
M_{\mathrm{Ch}}^{(d=5)} &= M_{\mathrm{Ch}}^{(0)}\left\{1 - C\frac{15}{16}\frac{R^5}{L^5}\right. \\
&\quad \left.\times\left[\frac{3\pi}{4}\frac{L^3}{R_E^3} - 3\frac{L^2}{R_E^2} + \frac{3}{2}\ln\left(\frac{2L}{R_E}\right) - \frac{1}{8}\right]\right\} \\
M_{\mathrm{Ch}}^{(d=6)} &= M_{\mathrm{Ch}}^{(0)}\left\{1 - C\frac{3}{2}\frac{R^6}{L^6}\right. \\
&\quad \left.\times\left[\frac{L^4}{R_E^4} - \frac{L^3}{R_E^3} + \frac{L}{2R_E} - \frac{35}{128}\right]\right\}.
\end{aligned} \tag{28}$$

Here the ordinary Chandrasekhar mass is

$$M_{\mathrm{Ch}}^{(0)} = \frac{15}{32\pi\mu^2 m_p^2}\sqrt{\frac{5h^3c^3}{2G^3}}. \tag{29}$$

In the calculations we have expanded in R^d to the first order. The corrections to the Chandrasekhar mass, that is the term proportional to R^d in eq. (28), must be small for the calculations to be valid.

By putting in the values of the constants in $M_{\mathrm{Ch}}^{(0)}$, with 2 decimals certainty one gets $M_{\mathrm{Ch}}^{(0)} \approx 3.4 \cdot 10^{30}$ kg. This could be compared with $1.3\, M_{Sun} \approx 2.6 \cdot 10^{30}$ kg mentioned in [2]. One probably should be satisfied with an order of magnitude right in this kind of calculations, because of the many assumptions one has had to make. Actually we are not so interested in getting a very exact value of $M_{\mathrm{Ch}}^{(0)}$ in this work (order of magnitude in the correction term is okay), since we only want to know if one is able to measure a difference from the normal Chandrasekhar mass.

Before we do numerical calculations to the corrections of the Chandrasekhar mass and put limits on how large and how many extra dimensions that is possible to have without contradicting existing astronomical observations of white dwarfs, we are also going to calculate the corrections to the maximum mass of a neutron star.

2.9 Neutron stars

A typical white dwarf has a characteristic density $\lesssim 10^{10}$ kg m^{-3} [2]. If the gas is compressed further than the characteristic density of the star, the kinetic energy of the electrons can become so large that protons and electrons by interactions may produce neutrons, in a process where energy is released. But as the number of electrons, that were providing the pressure for the gas, decreases the pressure does not build up rapidly enough and the star becomes unstable. The star will not be stable again until it reaches a central density of about 10^{16} kg m^{-3} [2]. When the star has reached this density, all the protons and electrons have united to neutrons. Neutrons are fermions and therefore obey Pauli's exclusion principle. The situation is quite similar to what we had for the electron gas. Therefore the same equations used for the electron gas in the white dwarf case can be used for the neutron gas.
But there are also important differences between a neutron star and a white dwarf. For example, a much higher density is required to push p_{F} up to the typical momentum of a neutron, which is more massive than an electron. Another difference is that there is no gas of ions providing most of the gravitation. In the neutron star, it is the neutrons themselves that contribute to the mass of the star. The mass contributions to the total mass of the star comes both from the rest mass and kinetic energy.

We will in the following cases assume that the neutron gas is in its lowest possible state, $T = 0$; that is the neutrons will occupy all the lowest momentum states up to the Fermi momentum p_{F}. This assumption makes the analysis of the neutron star easier. If $T > 0$ one would for example have to know the chemical potential for a neutron gas distribution, which is difficult to obtain.

2.9.1 A dense neutron star

Let us consider a very dense neutron star, where $p_{\mathrm{F}}c \gg m_n c^2$. We will basically have the same calculations as we had for the electron gas in the white dwarf. One can use the same number density equation and the same total (rest mass + kinetic)-energy equation as in the electron case, now of course considering neutrons instead of electrons. The neutrons are relativistic and they alone give the star its mass. Therefore one also has to count in the kinetic energy contribution to the total mass of the star.

We will now calculate E_n, the total (rest mass + kinetic)-energy of the neutron gas, in terms of the radius L and "rest mass" M of the star. By "rest mass" is meant the number of neutrons in the star times the rest mass m_n of one neutron. In another words, the total mass of all the neutrons in the star if they all were at rest.

$$
\begin{aligned}
E_n &= \rho_n V = V \int_0^{p_\mathrm{F}} \frac{8\pi p^2}{h^3}(m_n^2 c^4 + p^2 c^2)^{1/2} dp \\
&\approx V \int_0^{p_\mathrm{F}} \frac{8\pi p^3 c}{h^3} dp = V \frac{2\pi c}{h^3} p_\mathrm{F}^4 = \frac{2\pi V c}{h^3} n^{4/3} \left(\frac{3h^3}{8\pi}\right)^{4/3} \\
&= \left(\frac{3^5 h^3 c^3}{2^{11}\pi^2 m_n^4}\right)^{1/3} \frac{M^{4/3}}{L}, \qquad (30)
\end{aligned}
$$

where ρ_n is the total (rest mass + kinetic)-energy density of the neutron gas.

2.9.2 The maximum mass of a neutron star

We now seek $M_{max}^{(d)}$, which in our case means the maximal "rest mass" M of a neutron star with some radius L. As before d marks the number of extra space dimensions. The maximum mass can be found in the same as the white dwarf case, by an analysis of the total energy of the star:

$$
E_{tot}^{(d)} = E_n + E_{pot}^{(d)}. \qquad (31)
$$

We will assume as in the white dwarf case that the total energy of the star goes up again when the radius L becomes large in the non-relativistic range (not satisfying inequality (32) below). This means that if we have a maximum of $E_{tot}^{(d)}$ for smaller values of L in the relativistic range, the neutron star can have a minimum point somewhere between this maximum point and where the curve goes up again.

Let us consider a neutron star with radius L. As in the white dwarf case $p_\mathrm{F} c \gg m_n c^2$ (rewritten below) must be satisfied, as we are assuming a dense neutron gas (compare with what we had in the white dwarf case):

$$
L \ll \beta M^{1/3} \text{ where } \beta = \frac{h}{m_n c}\left(\frac{9}{32\pi^2 m_n}\right)^{1/3}. \qquad (32)
$$

By using the same kind of reasoning as in the white dwarf case we can get the maximum mass of the neutron star. But we need to replace M by (E_n/c^2) in $E_{pot}^{(d)}$ (eq. (17)), to account for the kinetic energy contribution to the mass. Also the neutron star will now cool instead for example by emitting neutrinos, and can in this way move down the energy curve and become a stable neutron star. We obtain $M_{max}^{(d)}$ in the same way as for the white dwarf, that is the partial derivative of $E_{tot}^{(d)}$, with respect of L (keeping M fixed) should be zero. From this condition to be satisfied one gets a relation between M and L. In the calculations we use that the correction terms in $E_{pot}^{(d)}$ are small and expand to first order in the term containing R^d. The result is the corrections to the maximum mass when $d = 0$:

$$
\begin{aligned}
M_{max}^{(d=1)} &= M_{max}^{(0)}\left\{1 - C\frac{15}{8}\frac{R}{L}\right\} \\
M_{max}^{(d=2)} &= M_{max}^{(0)}\left\{1 - C\frac{5}{12}\frac{R^2}{L^2}\left[\frac{15}{2}\ln\left(\frac{4L}{R_E}\right) - 19\right]\right\} \\
M_{max}^{(d=3)} &= M_{max}^{(0)}\left\{1 - C\frac{5}{32}\frac{R^3}{L^3}\left[\frac{5\pi L}{R_E} - 18\ln\left(\frac{2L}{R_E}\right) + 3\right]\right\} \\
M_{max}^{(d=4)} &= M_{max}^{(0)}\left\{1 - C\frac{5}{192}\frac{R^4}{L^4}\left(\frac{40L^2}{R_E^2} - \frac{72L}{R_E} + 63\right)\right\} \\
M_{max}^{(d=5)} &= M_{max}^{(0)}\left\{1 - C\frac{5}{384}\frac{R^5}{L^5}\right. \\
&\quad \left. \times\left[15\pi\frac{L^3}{R_E^3} - 54\frac{L^2}{R_E^2} + 24\ln\left(\frac{2L}{R_E}\right) - 1\right]\right\} \\
M_{max}^{(d=6)} &= M_{max}^{(0)}\left\{1 - C\frac{R^6}{1536L^6}\right. \\
&\quad \left. \times\left[\frac{640L^4}{R_E^4} - \frac{576L^3}{R_E^3} + \frac{256L}{R_E} - 135\right]\right\}.
\end{aligned}
\tag{33}
$$

Here is $M_{max}^{(0)}$ the rest mass, given by

$$
M_{max}^{(0)} = \left(\frac{2^{11}5^3c^9m_n^4\pi^2}{3^{11}G^3h^3}\right)^{1/4} L^{3/2} \tag{34}
$$

(Remember that M is the "rest mass" of the neutron star and not the observed mass. To get the real mass one has to know how relativistic the gas is. According to special relativity every neutron has an effective mass, which is the rest mass multiplied with the relativistic γ-factor. Instead of multiplying every neutron with its specific γ-factor, one can assume that there exist an average γ-factor for the gas. Then one can get the real mass of the neutron star by multiplying the "rest mass" with this average γ-factor. The mass corrections to $M_{max}^{(0)}$ would then be the same as in eq. (33), as the γ-factor would have come in on both sides of the equality sign.)

By using $L = 5 \cdot 10^3$ m, which is a reasonable value for a typical neutron star, and putting in the rest of the constants in $M_{max}^{(0)}$, with 2 decimals certainty, one gets $M_{max}^{(0)} = 4 \cdot 10^{30}$ kg $\approx 2\, M_{Sun}$. This is the order of magnitude value one is looking for, since the maximum mass of neutron star is somewhere between 1.5 and 2.5 solar masses, depending on the equation of state one uses.

2.10 Numerical calculations and conclusions

Newton's law for gravitation has been securely tested and confirmed down to lengths about 1 mm. (There has also been a recent test of the gravitational inverse-square law and no deviations has been found from Newtonian physics down to 218 μm [3].) So as a first upper limit on the size of the extra dimensions one has that $R \leq 1$ mm. But from recent experiments at LEP 2, CERN, one has got better upper limits on R when d is even [4]: $R^{(d=2)} = 4.8 \cdot 10^{-4}$ m, $R^{(d=4)} = 1.9 \cdot 10^{-11}$ m and $R^{(d=6)} = 6.8 \cdot 10^{-14}$ m.

One can also obtain upper limits to R_E in a white dwarf and a neutron star. Electrons and protons can interact and together they can form neutrons. In a white dwarf this happens roughly at kinetic energies equal to a few MeV, let us say 5 MeV. In a neutron star the neutrons do not remain particles for energies larger than, let us say 1 GeV. The effect of R_E in the potential is that it neglects contributions to the potential energy, when particles comes closer than R_E. Therefore we set R_E^{-1}, in corresponding energy units, equal to 5 MeV for the white dwarf and 1 GeV for the neutron star. For a white dwarf we then have $R_E = 4 \cdot 10^{-14}$ m and for the neutron star $R_E = 2 \cdot 10^{-16}$ m.

Star type	d	R (m)	$K^{(d)}$
White Dwarf	2	$4.8 \cdot 10^{-4}$	$7 \cdot 10^{-19}$
White Dwarf	4	$1.9 \cdot 10^{-11}$	$9 \cdot 10^{-31}$
White Dwarf	6	$6.8 \cdot 10^{-14}$	$1 \cdot 10^{-40}$
Neutron Star	2	$4.8 \cdot 10^{-4}$	$2 \cdot 10^{-13}$
Neutron Star	4	$1.9 \cdot 10^{-11}$	$1 \cdot 10^{-20}$
Neutron Star	6	$6.8 \cdot 10^{-14}$	$6 \cdot 10^{-26}$

Table 1: $K^{(d)}$ for a white dwarf and a neutron star when $d = 2, 4, 6$.

Let us now put in some standard values of the constants of a typical white dwarf and neutron star, to see if the change in the maximum mass is measurable. The best certainty one can accomplish today in astronomical measurements of the mass of white dwarfs and neutron stars, is roughly about 2 or 3 significant digits. So the corrections to the maximum mass, due to the existence of extra dimensions, must be better than this if one should be able to measure a difference.
As a typical radius for a white dwarf we use $L = 5000$ km and for a neutron star $L = 5$ km. For the rest of the constants we use the following values: $\mu = 2$, $h = 6.63 \cdot 10^{-34}$ J s, $G = 6.67 \cdot 10^{-11}$ N m^2 kg^{-2}, $m_n \approx m_p = 1.67 \cdot 10^{-27}$ kg and $c = 3.00 \cdot 10^8$ m s^{-1}.
If one defines the change in ratio of the maximum mass as $K^{(d)} \equiv 1 - M_{max}^{(d)}/M_{max}^{(0)}$, then one gets the result in table 1.

Thus our conclusion is that when d is even, the change in the maximum mass of a white dwarf or a neutron star is too small to be measurable.

3 Narrow Graviton Resonances at ATLAS

As mentioned in the introduction, we are in this second part going to investigate a possibility of finding signs of the spectrum of narrow (relative to the experimental resolution) massive graviton resonances that the Randall-Sundrum model predicts. The Randall-Sundrum model considers a space with only one very small extra dimension ($R \approx 10^{-32}$ m).

If gravitons can be generated from quarks and gluons, one should be able to find signs of that in experiments by studying particle collisions. This has been studied in [5] by looking at the characteristic angle distribution of outgoing electrons from the decayed graviton. It was shown in this article that it is difficult to make any conclusive statements from this experiment alone. To be convinced that the graviton exists, one therefore needs more experimental data that confirms the theories that predict its existence. On the following pages we will present a complementary measurement that can be made in the collision experiment. We will study the average value of $p_\perp$ of the graviton (see the section below) as a function of the graviton mass. The result can be compared with what one gets from the real experiment, to see if the predictions of the Randall-Sundrum model is correct.

3.1 The $p_\perp$-spectrum

We will now consider a collision experiment between highly energetic protons, which enables the partons (quarks and gluons) making up the proton to interact. A gluon-gluon pair (gg) and a quark-antiquark pair ($q\bar{q}$) can by fusion generate a graviton [8]. Because the incoming gluons and quarks are very energetic they will, due to QCD effects, radiate a lot of partons before they fuse together. This effect is called parton showering.

The two protons, and also the two incoming partons to be fused, are assumed to move in opposite directions with the same momentum magnitude when they come into the detector. If one looks at the situation from the partonic center of mass system, the generated graviton must be at rest after the fusion. But if one has parton showering, then the incoming partons may have changed their momentum before they fuse. If this is the case, the graviton can move along another direction than the original direction of the protons. So the graviton can have a transverse momentum magnitude $p_\perp$. By transverse is meant, perpendicular to the initial proton-proton motion direction.

Different interaction processes give rise to different $p_\perp$-spectrums, so we expect the initial pairs gg and $q\bar{q}$ to have different characteristic $p_\perp$-spectrums. We will in this work present a $p_\perp$-spectrum obtained from the event generator Pythia 6.1 [6], that could be compared with a measured $p_\perp$-spectrum. We will do our simulations for the planned ATLAS detector at CERN. Corresponding experiments are also planned for the CMS detector.

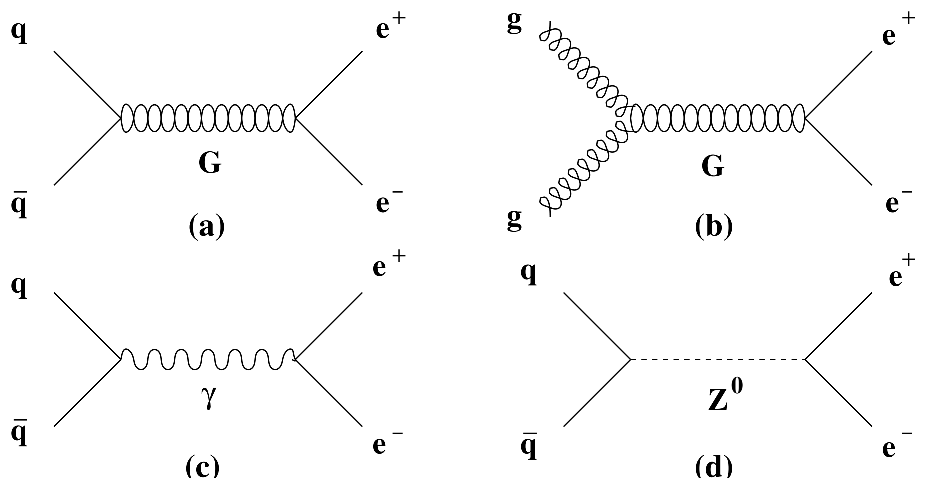

Figure 5: The relevant subprocesses for the signal and Standard Model background, for the graviton resonance production.

3.2 Cross sections and decay widths

Since the ATLAS detector has excellent energy and angular resolution for high energy electrons, we will consider subprocesses that have electrons in the final state. The relevant subprocesses, where the intermediate particle is a graviton G, are shown in fig. 5 a,b. The relevant Standard model background subprocesses are shown in fig. 5 c,d.

One also has to consider the interference between the Standard model subprocesses. Their interference with the subprocess in fig. 5 a can be neglected, because of the large mass difference between the intermediate particles. This can be seen by considering the Mandelstam variable s (see definition below) in neighborhood of the point $s = m_G^2$. Here the amplitude belonging to the graviton subprocess is δ-function like and the amplitude belonging to the Standard model subprocesses can be considered as constant. The amplitude squared has an interference term that is small compared to the individual subprocesses squared amplitudes and can therefore be neglected. The Mandelstam variables are by definition $s = (k_1 + k_2)^2$ and $t = (k_1 - q_1)^2$, where k_1, k_2 are the 4-momenta of the incoming particles and q_1, q_2 are the 4-momenta of the outgoing particles, as shown in fig. 6.

The differential cross sections, with respect to the Mandelstam variable t, of the Feynman diagrams in fig. 5 a,b are, in accordance with [7, 8]:

$$\begin{aligned} \frac{d\sigma^{(a)}}{dt} &= \frac{\kappa^4 s^2}{6144\pi}\frac{1+10x+42x^2+64x^3+32x^4}{(s-m_G^2)^2+m_G^2\Gamma_G^2} \\ \frac{d\sigma^{(b)}}{dt} &= \frac{\kappa^4 s^2}{1024\pi}\frac{-x(1+x)(1+2x+2x^2)}{(s-m_G^2)^2+m_G^2\Gamma_G^2}. \end{aligned} \tag{35}$$

The coupling constant is set as in [5], $\kappa = \sqrt{2}\alpha_1 k/(\bar{M}_{\rm Pl} m_G)$, where $k/\bar{M}_{\rm Pl} = 0.01$ and

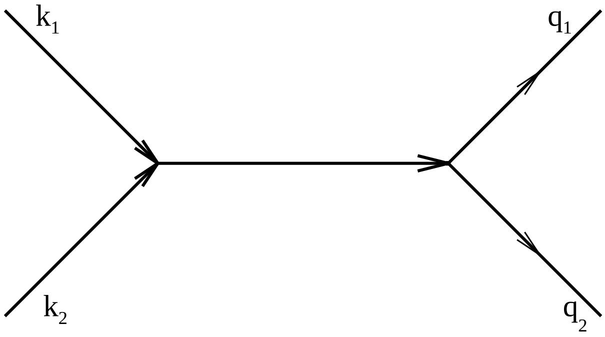

Figure 6: A Feynman diagram showing the 4-momenta mentioned in section 3.2.

$\alpha_1 = 3.8317$ is the first zero of the Bessel function $J_1(\alpha)$ of order 1. Higher zeros of the Bessel function give the other heavier graviton resonances that the Randall-Sundrum model predicts. In the analysis here we will however restrict ourself to the first one. m_G is the graviton mass, e_q is the quark charge and we set $x = t/s$ as in [7]. Γ_G is the total decay width of the graviton, given by the sum of the partial decay widths for the subprocesses. The partial decay widths are the same as in [8], with the correction given in [5]:

$$\begin{aligned}
\Gamma(G \to V\bar{V}) &= \delta \frac{\kappa^2 m_G^3}{80\pi}(1-4r_V)^{1/2}\left(\frac{13}{12}+\frac{14}{3}r_V+4r_V^2\right) \\
\Gamma(G \to f\bar{f}) &= N_c \frac{\kappa^2 m_G^3}{320\pi}(1-4r_f)^{3/2}\left(1+\frac{8}{3}r_f\right) \\
\Gamma(G \to gg) &= \frac{\kappa^2 m_G^3}{20\pi} \\
\Gamma(G \to \gamma\gamma) &= \frac{\kappa^2 m_G^3}{160\pi}.
\end{aligned} \tag{36}$$

N_c is the number of colors if there are any, otherwise $N_c = 1$. V stands for a massive vector boson ($V = Z^0, W^\pm$) with mass m_V. f stands for a fermion with mass m_f. $r_V = m_V^2/m_G^2$ and $r_f = m_f^2/m_G^2$. For identical particles $\delta = 1/2$ and for distinguishable particles $\delta = 1$.

3.3 The event generator Pythia 6.1

We now want to find out if the effect of the added subprocesses with a narrow graviton resonance could be measured in the LHC ATLAS experiment. To do that we will use a realistic event generator, that generates sets of outgoing particles produced in high energy collisions between two incoming particles. The program we use is Pythia 6.1 [6], that has been developed at the theoretical physics department here in Lund.

The cross sections and decay widths given above are put into the event generator. The values of the graviton mass m_G and the coupling constant $\kappa m_G = \sqrt{2} x_1 k/\bar{M}_{\text{Pl}}$ can be set in the program. The angular distributions for the decays of G to a fermion pair, given in [5], were put into the program. All other decays are set to be isotropic.
Already included in the program are initial- and final-state QCD parton showers, underlying event activity (multiple interactions and beam remnants), fragmentation to hadrons and unstable particle decays.

3.4 A simulated experiment

Let us now analyze the $p_\perp$-spectrum from a simulated LHC ATLAS experiment. We choose the center of mass energy $E_{\text{cm}} = 14$ TeV. If the ATLAS detector should be able to detect electrons, they must have pseudo-rapidity $|\eta| < 2.5$ and the transverse energy $E_\perp$ should either be larger than 30 GeV for one electron or larger than 20 GeV for both electrons.

The high luminosity planned for the ATLAS detector is $L = 100$ fb^{-1} [9], corresponding to one year of LHC running at design luminosity. In the measurement one desires a good signal to noise ratio, where the background noise comes from Standard model processes. We will consider an ideal experiment, which means that we turn of the effect of the detector in the program. The broading of the signal peak is then only due to the uncertainty in energy of the graviton. It is uncertain because it only exists for a short time.

To have a typical small event contribution from the Standard model background and on the same time covering the largest part of the resonance peak one chooses a mass window around the resonance maximum that is $3 \cdot \Gamma_m$, where Γ_m is the Gaussian experimental resolution. We take the values of Γ_m from tab. 2 in [5], with linear extrapolated values for masses between those given in the table.

From PYTHIA 6.1 we got the two $p_\perp$-spectrums shown in fig. 7. The $p_\perp$-spectrums for the different subprocesses are plotted for the graviton masses $m_G = 500$ GeV and $m_G = 2000$ GeV. Shown on the y-axis is the differentiated cross section with respect to the transverse momentum. With an incoming current J_i of particles on a target with an area A, as seen by the particles, the cross section is given by

$$\sigma = \frac{\Delta N}{J_i \Delta t} \text{ where } J_i = \frac{\Delta N_i}{A \Delta t}, \tag{37}$$

where ΔN is the number of particles that have interacted with the target and ΔN_i is the number of incoming particles, during a time Δt.

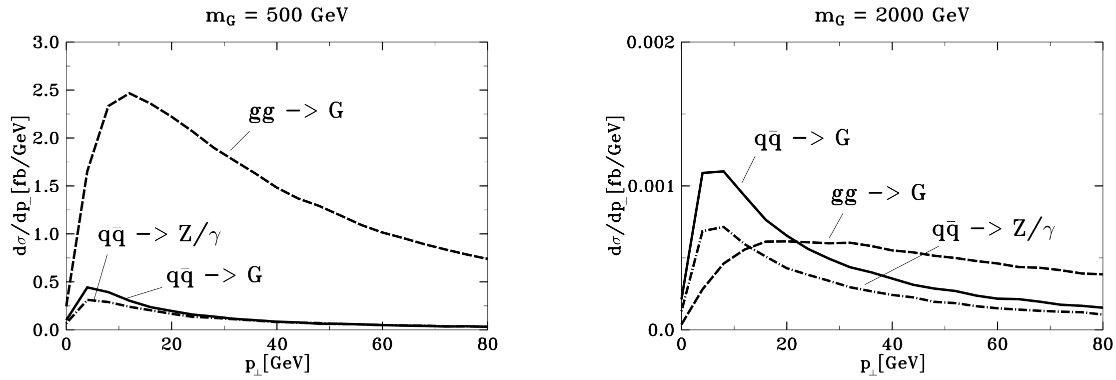

Figure 7: The $p_\perp$ spectrum for $m_G = 500$ GeV (left) and $m_G = 2000$ GeV (right). In the figure is shown the standard model background from γ, Z^0 production (dashed-dotted) line, the gg contribution (dashed line) and the $q\bar{q}$ contribution (solid line).

At least for the smaller graviton mass, $m_G = 500$ GeV, we see that the subprocess $gg \to G$ is the most prominent one, even if one compares it to the sum of the other two curves. Note that one from experiment does not get the three curves separately as shown in fig. 7, but the sum of the three curves. Notice also that the scale on the y-axis is much smaller for the larger mass, which means that the cross section is smaller for the larger mass.

3.5 The $p_\perp$-average for different graviton masses

Let us now consider another result that one can obtain by simulation. The average value of the transverse momentum magnitude $\sqrt{\langle p_\perp^2 \rangle}$, for some value of the graviton mass, is given by

$$\langle p_\perp^2 \rangle = \sigma^{-1} \cdot \int_0^\infty p_\perp^2 \frac{d\sigma}{dp_\perp} dp_\perp. \tag{38}$$

We now run Pythia 6.1 several times with different graviton masses. The result is shown in fig. 8, where $\sqrt{\langle p_\perp^2 \rangle}$ is plotted as a function of the graviton mass. The full circles show the average $p_\perp$-values for the subprocess $gg \to G$, the open circles show the average $p_\perp$-values for the $q\bar{q} \to G$ subprocess and the squares show the Standard model background. The triangles show the total average $p_\perp$-values of both subprocesses above, including the Standard model subprocesses. We see that for smaller values of m_G the process $gg \to G$ is much more dominant than the other processes.

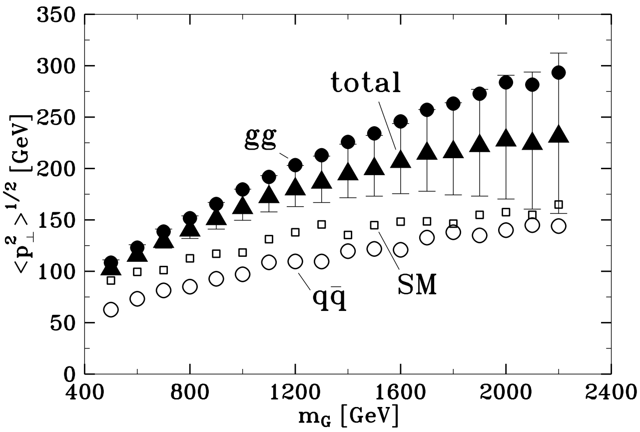

Figure 8: $\sqrt{\langle p_\perp^2 \rangle}$ plotted as a function of the graviton mass. The full circles show the average $p_\perp$-values for the subprocess $gg \to G$, the open circles show the average $p_\perp$-values for the $q\bar{q} \to G$ subprocess and the squares show the Standard model background. The triangles show the total average $p_\perp$-values for all subprocesses. The error bars are also put in for the total average $p_\perp$-values for $L = 100$ fb^{-1}.

For the relative errors of the total average of $p_\perp$ we take:

$$\left(\frac{\Delta p_\perp}{p_\perp}\right)^2 = (\sigma L)^{-1} + (5 \cdot 10^{-4}\, p_\perp \mathrm{GeV}^{-1})^2 + (0.02)^2, \tag{39}$$

for a luminosity $L = 100$ fb^{-1}. The errors are shown as error bars in fig. 8.

3.6 Conclusions

In a proton-proton collision there is a possibility for the partons to produce massive graviton states by fusion processes. If this is the case, one could find signs of that in the characteristic $p_\perp$-spectrums of the subprocesses. We obtained the $p_\perp$-spectrums by simulating an experiment for the upcoming ATLAS detector at LHC, with the event generator Pythia 6.1. The points in fig. 8 show the ideal case where the detector does not affect the results. These curves are predicted by the Randall-Sundrum model and can be compared with the curves that one gets from experiment. On the total $p_\perp$-average is added error bars to show the relative statistical error one would have, if the measured curve would be the triangular one, for a luminosity of $L = 100$ fb^{-1}.

References

[1] R. Casadio and B. Harms, Phys. Lett. **B487**, 209 (2000) [hep-th/0004004].

[2] F. Schutz, *A first course in general relativity*, Cambridge University Press 1990.

[3] C. D. Hoyle, U. Schmidt, B. R. Heckel, E. G. Adelberger, J. H. Gundlach, D. J. Kapner and H. E. Swanson, hep-ph/0011014.

[4] I. Antoniadis and K. Benakli, hep-ph/0007226.

[5] B. C. Allanach, K. Odagiri, M. A. Parker and B. R. Webber, JHEP **0009**, 019 (2000) [hep-ph/0006114].

[6] T. Sjostrand, P. Eden, C. Friberg, L. Lonnblad, G. Miu, S. Mrenna and E. Norrbin, hep-ph/0010017.

[7] G. F. Giudice, R. Rattazzi and J. D. Wells, Nucl. Phys. **B544**, 3 (1999) [hep-ph/9811291].

[8] T. Han, J. D. Lykken and R. Zhang, Phys. Rev. **D59**, 105006 (1999) [hep-ph/9811350].

[9] "ATLAS: Detector and physics performance technical design report. Volume 1," CERN-LHCC-99-14.